Eur. Phys. J. A **16**, 387–392 (2003)
DOI 10.1140/epja/i2002-10050-8

THE EUROPEAN PHYSICAL JOURNAL A

Single-particle quadrupole electromagnetic transitions in p-shell and sd-shell nuclei

R.A. Radhi[a]

Department of Physics, College of Science, University of Baghdad, Baghdad, Iraq

Received: 18 April 2002 / Revised version: 28 June 2002 /
Published online: 6 March 2003 –
Communicated by A. Molinari

Abstract. Electron scattering Coulomb form factors for the single-particle quadrupole transitions in p-shell and sd-shell nuclei have been studied. Core polarization effects are included through a microscopic theory that includes excitations from the core orbits up to higher orbits with $2\hbar\omega$ excitations. The modified surface delta interaction is adopted as a residual interaction. The results are discussed for the $(1p_{1/2}^{-1} \rightarrow 1p_{3/2}^{-1})$ proton transition in ^{15}N, $(1d_{5/2} \rightarrow 2s_{1/2})$ neutron transition in ^{17}O and $(1d_{3/2}^{-1} \rightarrow 2s_{1/2}^{-1})$ proton transition in ^{39}K. The inclusion of core polarization effects modifies the form factors markedly and describes the experimental data very well in both the absolute strength and the momentum transfer dependence.

PACS. 25.30.Dh Inelastic electron scattering to specific states – 21.60.Cs Shell model – 27.20.+n $5 \leq A \leq 19$ – 27.40.+z $39 \leq A \leq 58$

Introduction

Shell model calculations, carried out within a model space in which the nucleons are restricted to occupy a few orbits are able to reproduce the measured transition strengths when appropriate effective charges for the protons and neutrons are used. The Coulomb form factors have been discussed for the stable sd-shell nuclei using sd-shell wave functions with phenomenological effective charges [1]. However, the introduction of effective charges may bring the calculated transition strengths, which are defined at the photon point, as well as, the form factors at the first maximum, closer to the measured values, but the non-zero momentum transfer (q) values might deviate appreciably from the measured values. For electric quadrupole excitations, it has been recognized that these transitions have highly collective properties. To supplement usual shell model treatments, core polarization calculations based on a microscopic theory provide a more practical attempt to describe such collective Coulomb quadrupole excitations. Core polarization effects have been calculated by using microscopic models for transition between single-particle (or hole) states with LS closed shell [2]. A microscopic model has been used [3] to study the core polarization effect on the transition and current densities of single-particle configurations. Their model gave quite satisfactory results for describing the quadrupole core polarization charges in the sd-shell nuclei in comparison with the empirical ones. Moreover, the Coulomb form factor of the $(1d_{3/2}^{-1} \rightarrow 2s_{1/2}^{-1})$ transition in ^{39}K gave a remarkably good agreement with experimental form factors both in the absolute strength and the q-dependence [3]. Core polarization effects were taken into account by Arima *et al.* [4] in the study of the magnetic form factor of ^{17}O. The first-order core polarization effects were incorporated with the p-shell wave functions by Sato *et al.* [5], where these effects greatly improved the agreement with the experimental (e, e'), (π, π') and (γ, π) data from ^{10}B. The inclusion of higher-excited configurations by means of core polarization calculations was essential to remove the shortfall in describing electron scattering form factors of ^{10}B [6].

In the present work, the $C2$ longitudinal form factors are studied for ^{15}N, ^{17}O and ^{39}K. The nuclei ^{15}N and ^{39}K represent a proton hole inside a closed shell, while ^{17}O represents a neutron particle outside a closed shell. Higher-energy configurations are included as a first-order core polarization through a microscopic theory which combines shell model wave functions and highly excited states. Single-particle wave functions are used as a zero-th contribution and the effect of core polarization is included as a first-order perturbation theory with the modified surface delta interaction (MSDI) [7] as a residual interaction and a $2\hbar\omega$ for the energy denominator. The single-particle wave functions are those of the harmonic-oscillator (HO) potential with size parameter b chosen to reproduce the measured root mean square (rms) charge radii of these nuclei.

[a] e-mail: baguniv@uruklink.net

Theory

The core polarization effect on the form factors is based on a microscopic theory, which combines shell model wave functions and configurations with higher energy as first-order perturbations; these are called core polarization effects. The reduced matrix elements of the electron scattering operator T_Λ is expressed as the sum of the product of the elements of the one-body density matrix (OBDM) $\chi^{\Lambda}_{\Gamma_\mathrm{f}\Gamma_\mathrm{i}}(\alpha,\beta)$ times the single-particle matrix elements, and is given by

$$\langle \Gamma_\mathrm{f}|||T_\Lambda|||\Gamma_\mathrm{i}\rangle = \sum_{\alpha,\beta} \chi^{\Lambda}_{\Gamma_\mathrm{f}\Gamma_\mathrm{i}}(\alpha,\beta)\,(\alpha|||T_\Lambda|||\beta)\ , \qquad (1)$$

where α and β label single-particle states (isospin is included) for the model space. For p-shell nuclei, the orbits $1p_{3/2}$ and $1p_{1/2}$ define the model space. For the sd-shell, the orbits $1d_{5/2}$, $2s_{1/2}$ and $1d_{3/2}$ define the model space. The states $|\Gamma_\mathrm{i}\rangle$ and $|\Gamma_\mathrm{f}\rangle$ are described by the model space wave functions. Greek symbols are used to denote quantum numbers in coordinate space and isospace, *i.e.* $\Gamma_\mathrm{i} \equiv J_\mathrm{i}T_\mathrm{i}$, $\Gamma_\mathrm{f} \equiv J_\mathrm{f}T_\mathrm{f}$ and $\Lambda \equiv JT$.

According to the first-order perturbation theory, the single-particle matrix element is given by [7]

$$(\alpha|||T_\Lambda|||\beta) = \langle\alpha|||T_\Lambda|||\beta\rangle + \langle\alpha|||T_\Lambda\frac{Q}{E_\mathrm{i}-H_0}V_\mathrm{res}|||\beta\rangle + \langle\alpha|||V_\mathrm{res}\frac{Q}{E_\mathrm{f}-H_0}T_\Lambda|||\beta\rangle\ . \qquad (2)$$

The first term is the zeroth-order contribution. The second and third terms are the core polarization contributions. The operator Q is the projection operator onto the space outside the model space. For the residual interaction, V_res, we adopt the MSDI (7). E_i and E_f are the energies of the initial and final states, respectively. The core polarization terms are written as [7]

$$\sum_{\alpha_1\alpha_2\Gamma} \frac{(-1)^{\beta+\alpha_2+\Gamma}}{e_\beta - e_\alpha - e_{\alpha_1} + e_{\alpha_2}}(2\Gamma+1)\left\{\begin{matrix}\alpha & \beta & \Lambda\\ \alpha_2 & \alpha_1 & \Gamma\end{matrix}\right\} \times\sqrt{(1+\delta_{\alpha_1\alpha})(1+\delta_{\alpha_2\beta})} \times\langle\alpha\alpha_1|V_\mathrm{res}|\beta\alpha_2\rangle_\Gamma\langle\alpha_2|||T_\Lambda|||\alpha_1\rangle + \text{terms with } \alpha_1 \text{ and } \alpha_2 \text{ exchanged with an overall minus sign}\,, \qquad (3)$$

where the index $\alpha_1$runs over particle states and α_2 over hole states and e is the single-particle energy. The core polarization parts are calculated by keeping the intermediate states up to the $2p1f$-shell for ^{15}N and ^{17}O. For ^{39}K, the intermediate states are kept up to $1g3s2d$-shell.

The single-particle matrix element reduced in both spin and isospin is written in terms of the single-particle matrix element reduced in spin only [7]

$$\langle\alpha_2|||T_\Lambda|||\alpha_1\rangle = \sqrt{\frac{2T+1}{2}}\sum_{t_z} I_T(t_z)\langle\alpha_2||T_{Jt_z}||\alpha_1\rangle \qquad (4)$$

with

$$I_T(t_z) = \begin{cases} 1\,, & \text{for } T=0\,,\\ (-1)^{1/2-t_z}\,, & \text{for } T=1\,,\end{cases} \qquad (5)$$

where $t_z = 1/2$ for a proton and $-1/2$ for a neutron.

The reduced single-particle matrix element of the Coulomb operator is given by [8]

$$\langle\alpha_2||T_J||\alpha_1\rangle = \int_0^\infty \mathrm{d}r r^2 j_J(qr)\langle\alpha_2||Y_J||\alpha_1\rangle R_{n_1\ell_1}(r)R_{n_2\ell_2}(r), \qquad (6)$$

where $j_J(qr)$ is the spherical Bessel function and $R_{n\ell}(r)$ is the single-particle radial wave function.

Electron scattering form factor involving angular momentum J and momentum transfer q, between the initial and final nuclear shell model states of spin $J_\mathrm{i,f}$ and isospin $T_\mathrm{i,f}$ is [9]

$$|F_J(q)|^2 = \frac{4\pi}{Z^2(2J_\mathrm{i}+1)}\left|\sum_{T=0,1}\begin{pmatrix} T_\mathrm{f} & T & T_\mathrm{i}\\ -T_z & 0 & T_z\end{pmatrix} \times\langle J_\mathrm{f}T_\mathrm{f}|||T_{JT}|||J_\mathrm{i}T_\mathrm{i}\rangle\right|^2 F^2_\mathrm{cm}(q)F^2_\mathrm{fs}(q)\,, \qquad (7)$$

where T_z is the projection along the z-axis of the initial and final isospin states and is given by $T_z = (Z-N)/2$. The nucleon finite-size (fs) form factor is $F_\mathrm{fs}(q) = \exp(-0.43q^2/4)$ and $F_\mathrm{cm}(q) = \exp(q^2b^2/4A)$ is the correction for the lack of translational invariance in the shell model. A is the mass number, and b is the harmonic-oscillator size parameter.

The single-particle energies are calculated according to [7]

$$e_{nlj} = (2n+l-1/2)\hbar\omega + \begin{cases} -\frac{1}{2}(l+1)\langle f(r)\rangle_{nl}\,, & \text{for } j=l-1/2\,,\\ \frac{1}{2}l\langle f(r)\rangle_{nl}\,, & \text{for } j=l+1/2\,,\end{cases} \qquad (8)$$

with $\langle f(r)\rangle_{nl} \approx -20A^{-2/3}$ and $\hbar\omega = 45A^{-1/3} - 25A^{-2/3}$.

Results and discussion

The core polarization effects are calculated with the MSDI as a residual interaction. The strength parameters of the MSDI are denoted by A_T, B *and* C [7], where T indicates the isospin (0,1). An empirical estimate of these parameters can be obtained as a function of the mass number A by comparing the calculated quadrupole moments for the stable sd-shell nuclei with $J^\pi = 3/2^+$ and $5/2^+$ using core polarization effects with the measured values. The model space wave functions in this case are no longer single-particle wave functions. We use the wave functions of Chung-Wildenthal interactions, where the OBDM are taken from ref. [10]. The results of such comparison gives the values of the parameters equal to $A_0 = A_1 = B = (20/A)$ MeV and $C = 0$. The measured qudrupole moments for these nuclei are well described as

Table 1. Electric ground-state quadrupole moment Q (in units of $e \cdot \text{fm}^2$).

				Q		
Nucleus	J^π	T	b (fm)[a]	No CP	With CP	Experiment[b]
^{17}O	$5/2^+$	1/2	1.763	0.0	-2.84	-2.58
^{21}Ne	$3/2^+$	1/2	1.845	5.77	9.87	10.3 ± 0.8
^{23}Na	$3/2^+$	1/2	1.810	5.92	9.62	10.8 ± 0.8
^{25}Mg	$5/2^+$	1/2	1.793	11.10	16.36	22
^{27}Al	$5/2^+$	1/2	1.804	8.96	12.30	14.0 ± 0.02
^{33}S	$3/2^+$	1/2	1.881	-3.76	-5.89	-6.4 ± 1.0
^{35}Cl	$3/2^+$	1/2	1.921	-4.67	-6.82	-8.2
^{37}Cl	$3/2^+$	3/2	1.921	-5.0	-5.63	-6.5
^{39}K	$3/2^+$	1/2	1.950	5.32	7.12	5.4 ± 0.2

([a]) Table 3 in ref. [10].
([b]) Refs. [11–13].

Table 2. Theoretical calculations of the reduced transition probabilities $B(C2\uparrow)$ values (in units of $e^2 \cdot \text{fm}^4$) in comparison with experimental values.

				$B(C2\uparrow)$			
Nucleus	J_f^π	T_f	(E_x MeV)	s.p.	s.p. + CP	s.p. (with e_eff)	Exp.
^{15}N	$3/2^-$	1/2	(6.32)	7.87	15.14	14.35	14.80 ± 5.0[a]
^{17}O	$1/2^+$	1/2	(0.87)	0.0	2.02	2.12	2.18 ± 0.16[b]
^{39}K	$1/2^+$	1/2	(2.53)	11.5	22.72	20.92	18.90 ± 1.8[c]

([a]) Ref. [15].
([b]) Ref. [18].
([c]) Ref. [17].

Table 3. The one-body density matrix elements.

Nucleus	J_f^π	T_f	α	β	$\chi^{20}_{\Gamma_\text{f}\Gamma_\text{i}}(\alpha,\beta)$	$\chi^{21}_{\Gamma_\text{f}\Gamma_\text{i}}(\alpha,\beta)$
^{15}N	$3/2^-$	1/2	$1p_{1/2}$	$1p_{3/2}$	1.0	-1.0
^{17}O	$1/2^+$	1/2	$1d_{5/2}$	$2s_{1/2}$	1.0	1.0
^{39}K	$1/2^+$	1/2	$1d_{3/2}$	$2s_{1/2}$	1.0	-1.0

given in table 1. This choice of the strength parameters brings the calculated $B(C2\uparrow)$ values for the transitions to the states $3/2^-1/2$ (6.32 MeV), $1/2^+1/2$ (0.87 MeV) and $1/2^+1/2$ (2.53 MeV) in ^{15}N, ^{17}O and ^{39}K, respectively, very close to the measured values as shown in table 2. The single-particle wave functions are those of the HO potential whose size parameters b are chosen to reproduce the measured rms charge radii and are displayed in table 1. The OBDM elements for the transitions considered in this work for ^{15}N, ^{17}O and ^{39}K are given in table 3.

The $C2$ form factors for the $3/2^-1/2$ state at excitation energy $E_x = 6.32$ MeV of ^{15}N are shown in fig. 1(a). The dashed curve represents the calculation with the single-particle (s.p.) model ($1p^{-1}_{1/2} \rightarrow 1p^{-1}_{3/2}$). The oscillator parameter b is taken to be 1.678 fm to reproduce the rms charge radius [14]. The calculated $B(C2\uparrow)$ value is found to be equal to 7.87 $e^2 \cdot \text{fm}^4$ in comparison with the measured value 14.8 ± 5.0 [15]. The data are well described by this model for $q > 1.5$ fm^{-1}, while the low-q data as well as the photon point are underestimated. The core polarization effects are included by allowing particle-hole excitations form $1s$ and $1p$ shells up to the higher shells with $2\hbar\omega$ excitations. The core polarization form factor (CP) is shown by the dotted curve. The full calculations that include core polarization effects (s.p. + CP) are shown by the solid curve. The inclusion of core polarization effects enhances the form factor for $q < 1.5$ fm^{-1} and brings the photon point very close to the measured value as given in table 2. An excellent overall agreement is obtained with the measured data. When we use effective charge ($e_\text{eff} = 1.35\ e$) for the valence proton to reproduce the measured $B(C2\uparrow)$ value, the calculations agrees very well with those which include the core polarization effects, only for $q < 1.0$ fm^{-1}. These calculations are shown by the cross symbols in fig. 1(b) in comparison with the s.p. model (dashed curve) and with the full calculations that include core polarization effects (solid curve). The constant effective charge cannot explain the data for $q > 1.0$ fm^{-1}. The core polarization calculations show that the effective charge must be q-dependent in order to fit the data in the different q regions. In comparison with the results of ref. [2], the Rosenfeld result (RM) described the data only for $q \leqslant 1.0$ fm^{-1}, and this result looks like the effective-charge result given in fig. 1(b) as a cross symbols curve. The G-matrix result (KR) slightly overshoots the data. The attractive triple-odd interaction (ATO) gives almost same result as that used in the present

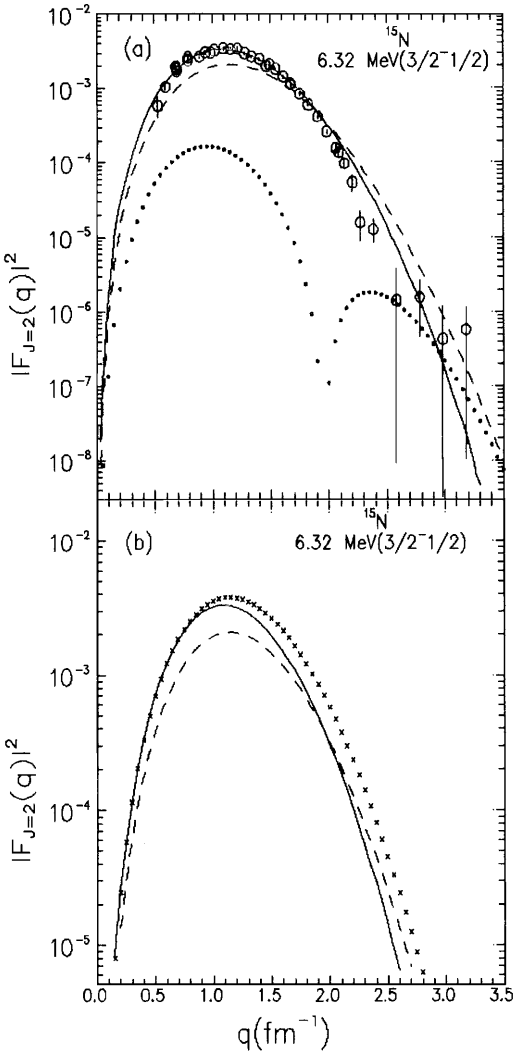

Fig. 1. The Coulomb form factor of the quadrupole transition to the $3/2^-1/2$ state in ^{15}N. The upper panel (a) represents the calculations of the single-particle model without core polarization effects (dashed curve) and with core polarization effects (solid curve). The dotted curve in (a) represents the core polarization contribution. The data are taken from ref. [19]. The lower panel (b) represents the comparison between the effective-charge model (cross symbols) with the single-particle model which includes core polarization (solid curve) and also with that which does not include core polarization (dashed curve).

work. However, ref. [2] used a size parameter b for the HO potential equal to 1.7 fm which is in between the value used in this work ($b = 1.678$ fm) to get the rms charge radius and the value that adjusted to the elastic electron scattering on ^{15}N which is equal to 1.74 fm [16].

The $C2$ form factor for the $1/2^+1/2$ state at $E_x = 0.817$ MeV of ^{17}O are shown in fig. 2. The zeroth-order calculations give no contribution to the $C2$ form factor, since the s.p. model represents a neutron outside a closed $1p$-shell. The inclusion of core polarization effects reproduces the measured $B(C2\uparrow)$ value correctly, as given in

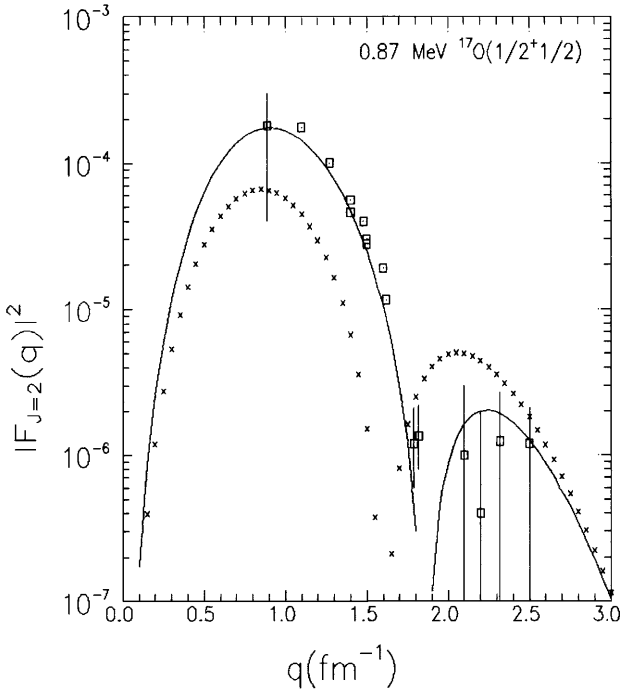

Fig. 2. The Coulomb form factor of the quadrupole transition to the $1/2^+1/2$ state in ^{17}O. The solid curve corresponds to the single-particle model with core polarization. The cross symbols correspond to the single-particle model with effective charges. The data are taken from ref. [18].

table 2, and describe the non-zero q-values very well, reproduces the first and second maxima, and locates the diffraction minimum at its right location, as shown by the solid curve in fig. 2. The effective-charge model reproduces the measured $B(C2\uparrow)$ value with $e_{\rm eff} = 0.525\ e$ for the valence neutron, and the non-zero q-values deviate significantly from the core polarization calculations and hence the experimental data, as shown by the cross symbols in fig. 2. The effective-charge model underestimates the data for the first maximum by about a factor of 2, while overpredicts the second maximum by an order of magnitude. In comparison with the result of ref. [2], the G-matrix result underestimates the data for the first maximum by a factor of 4. The data for the second maximum have large error bars. The ATO result gives the first maximum at about $8 \times 10^{-5}\ e^2 \cdot {\rm fm}^4$, while the data gives the value $\approx 2 \times 10^{-4}\ e^2 \cdot {\rm fm}^4$, for the form factor. The location of the diffraction minimum and the form factor values for the second maximum agree very well with our results. The RM result underestimated the data for the first maximum by about a factor of 3, while the second maximum overestimated the data by a factor of more than 3. Also, the location of the diffraction minimum was shifted towards a value of q lower than that of the ATO and our results. The RM result gave the same behavior as the effective-charge result (cross symbols curve in fig. 2).

The $C2$ form factors for the $1/2^+1/2$ state at $E_x = 2.53$ MeV of ^{39}K are shown in fig. 3(a). The single-particle (s.p.) model ($1d_{3/2}^{-1} \rightarrow 2s_{1/2}^{-1}$) (dashed curve)

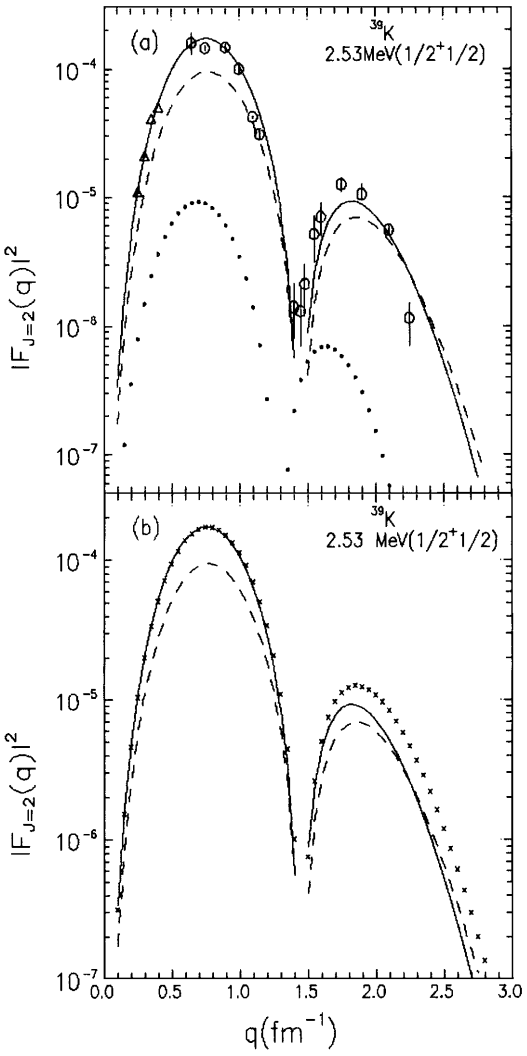

Fig. 3. The Coulomb form factor of the quadrupole transition to the $1/2^+1/2$ state in ^{39}K. The upper panel (a) represents the calculations of the single-particle model without core polarization effects (dashed curve) and with core polarization effects (solid curve). The dotted curve in (a) represents the core polarization contribution. The data are taken from ref. [17] (triangles), ref. [20] (circles). The lower panel (b) represents the comparison between the effective-charge model (cross symbols) with the single-particle model which includes core polarization (solid curve) and also with that which does not include core polarization (dashed curve).

underestimates the data in both the transition strength ($11.5\ e^2 \cdot \mathrm{fm}^4$ in comparison with the measured value $18.9 \pm 1.8\ e^2 \cdot \mathrm{fm}^4$ [17]) and the q-dependent form factor. The core polarization effects are calculated by allowing particle-hole excitations from the core-orbits ($1s$, $1p$ and $2s1d$ shells) into the higher orbits with $2\hbar\omega$ excitations. The inclusion of core polarization effects reproduces the measured transition strength correctly as given in table 2 and describes the non-zero q-values very well as shown by the solid curve in fig. 3(a). Figure 3(b) shows the comparison between the effective charge model that using effective charge = 1.35 e, (cross symbols) and the s.p. model which includes core polarization (solid curve) and also with that which does not include core polarization (dashed curve). The effective-charge model gives almost the same result as the core polarization result for $q \leqslant 2$ fm^{-1}, and starts to deviate towards higher q-values beyond that.

Our result agrees very well with that of ref. [3], using Hatree-Fock single-particle wave functions and the particle-vibration-coupling model for core polarization calculations. The ATO result of ref. [2] agrees very well with our result in the region of the first maximum, while it underestimates the data by about a factor of 2 in the region of the second maximum. The RM and KR results in this case describe the data better than the ATO result in the region of the second maximum, but slightly underestimate the data in the region of the first maximum.

Conclusions

Core polarization effects are essential in the calculation of $C2$ form factors. The inclusion of core polarization gives a remarkable improvement in the form factors both in the absolute strengths and the momentum transfer dependence without introducing adjustable parameters. Effective-charge models cannot be always considered as a successful alternative for core polarization calculations. The MSDI, which has a simple form, used for the intermediate states, as a residual interaction between particles out of the model space is an adequate choice for core polarization calculations. Core polarization calculations presented in the present work, succeeded in describing the electron scattering data at the beginning of the sd-shell nuclei and at the end. These calculations can be extended to cover the entire sd-shell region, and also can be used even for higher shells.

References

1. B.A. Brown, R. Radhi, B.H. Wildenthal, Phys. Rep. **101**, 313 (1983).
2. Y. Horikawa, T. Hoshino, A. Arima, Nucl. Phys. A **278**, 297 (1977).
3. H. Sagawa, B.A. Brown, Nucl. Phys. A **430**, 84 (1984).
4. A. Arima, Y. Horikawa, H. Hyuga, T. Suzuki, Phys. Rev. Lett. **40**, 1001 (1978).
5. T. Sato, N. Odagawa, H. Ohtsubo, T.S.H. Lee, Phys. Rev. C **49**, 776 (1994).
6. A. Cichocki, J. Dubach, R.S. Hicks, G.A. Peterson, C.W. de Jager, H. de Vries, N. Kalantar-Nayestanaki, T. Sato, Phys. Rev. C **51**, 2406 (1995).
7. P.J. Brussaard, P.W.M. Glaudemans, *Shell Model Applications in Nuclear Spectroscopy* (North Holland, Amsterdam, 1977).
8. T. de Forest jr., J.D. Walecka, Adv. Phys. **15**, 1 (1966).
9. T.W. Donnelly, I. Sick, Rev. Mod. Phys. **56**, 461 (1984).
10. B.A. Brown, W. Chung, B.H. Wildenthal, Phys. Rev. C **22**, 774 (1980).

11. F. Ajzenberg-Selove, Nucl. Phys. A **281**, 1 (1977)
12. F. Ajzenberg-Selove, Nucl. Phys. A **300**, 1 (1978)
13. P.M. Endt, C. van der Leun, Nucl. Phys. A **235**, 27 (1974).
14. C.W. de Jager, H. de Vries, C. de Vries, At. Data Nucl. Data Tables **14**, 179 (1974).
15. G.A. Beer, D. Brix, H.G. Clerc, B. Laube, Phys. Lett. B **26**, 506 (1968).
16. E.B. Dally, M.G. Croisseaux, B. Schweitz, Phys. Rev. C **2**, 2057 (1970).
17. Grundy Th., Richter A, G. Schrieder, E. Spamer, W. Stock, Nucl. Phys. A **357**, 269 (1981).
18. D.M. Manley, B.L. Berman, W. Bertozzi, T.N. Butti, J.M. Finn, F.W. Hersman, C.E. Hyde-Wright, M.V. Hynes, J.J. Kelly, M.A. Kovash, S. Kowalski, R.W. Lourie, B. Murdock, B.E. Norum, B. Pugh, C.P. Sargent, Phys. Rev. C **36**, 1700 (1987).
19. J. Millener, private communication, from the thesis by J.W. de Vries, 1987.
20. C.W. de Jager, P.H.M. Keizer, S.W. Kowalski, L. Lapikas, E.A.J.M. Offermann, H. de Vries, in *Proceedings of the International Conference on Nuclear Physics, Contributed Papers, Florence, 1983*, edited by R.A. Ricci, P. Blasi, Vol. **1** (Tipografia Compositori, Bologna, 1983),